**Lili Chen**[1],
**Hongjun Guo**[2]

1 – Laboratory of Intelligent Information Processing, Suzhou University, Suzhou, China
2 – The Key Laboratory of Intelligent Computing & Signal Processing of MOE, Anhui University, Hefei, China

# A SIMPLE AND EFFICIENT FUSION FRAMEWORK FOR SURVEILLANCE IMAGES

**Лілі Чен**[1],
**Хунцзюнь Го**[2]

1 – Лабораторія інтелектуальної обробки інформації, Сучжоу університет, Сучжоу, Китай
2 – Лабораторія інтелектуальних обчислень і обробки сигналів Міністерства освіти, Аньхой університет, Хефей, Китай

# ПРОСТИЙ ТА ЕФЕКТИВНИЙ ФРЕЙМВОРК ЗЛИТТЯ ДЛЯ ЗОБРАЖЕНЬ З КАМЕР СПОСТЕРЕЖЕННЯ

**Purpose.** Aiming at solving the fusion issue of surveillance images, a simple and efficient fusion framework using block compressed sensing sampling (BCSS) is proposed in this paper, which consists of two fusion methods using basic-BCSS and sliding-BCSS respectively.

**Methodology.** With the superiority of low sampling ratio and low computational complexity, compressed sensing (CS) theory is widely used in signal processing. The basic-BCSS is a basic version of block based CS, in which the source image is divided into distinct blocks, and the sliding-BCSS is a modified version of basic-BCSS proposed for the first time, in which the image is divided into small sliding blocks for each pixel with appropriate padding. The basic idea of the fusion framework is to select the blocks or pixels with greater L2-norm of the BCSS measurement outputs of the divided blocks in spatial domain.

**Findings.** The fusion framework is tested on three pairs of grayscale surveillance images, including infrared and visible images, and millimeter-wave and visible images, and compared with several traditional fusion methods. Experimental results demonstrate that the proposed fusion framework can significantly improve the fusion quality and speed simultaneously.

**Originality.** A simple and efficient fusion framework using BCSS in spatial domain is proposed for the first time.

**Practical value.** It has a certain practical meaning for real-time surveillance applications.

**Keywords:** *image fusion, spatial domain, surveillance, infrared, block compressed sensing sampling, real-time*

**Introduction.** In surveillance applications, the design of sensors with better quality or some specific characteristics may be limited by technical constraints [1], and image fusion can fuse the information across the electromagnetic spectrum, such as infrared, near-infrared, millimeter-wave (MMW) and visible bands [1].

The widely used visible image reflects the characteristics of the targets in the visible band, and it is sensitive to the change of the brightness in the scene and accord with human visual perception [2, 3]. The infrared image is sensitive to the objects which have higher temperature than the background, which make it able to see at night without illumination, and the disadvantage is its poor spatial resolution [1]. The MMW image is widely used to detect objects concealed underneath a person's clothing using a form of electromagnetic radiation, and it usually have low contrast and higher noise. Image fusion can take full advantages of the different and complementary information from those images to make up for the limitation of one single sensor. The fusion of infrared and visible images also has been investigated for other surveillance problems in recent years, such as image dehazing, face recognition and many military reconnaissance [1].

In response to the requirements in real-time surveillance applications, the experts and scholars pay much attention in proposing more effective fusion methods. The methods are usually categorized into two basic groups: the spatial domain methods and the frequency domain based methods.

In spatial domain, the fusion methods are generally directly functioned on the pixels. The simplest method is to take the average of the source images pixel by pixel, which is known as spatial average (SA) method. An often mentioned principal component analysis (PCA) based fusion method mainly adopts the idea of the so-called 'component substitution', which is not suitable for fusion of two grayscale images and is usually used in remote sensing image fusion. The Matlab code of PCA based fusion method provided by Oliver Rockinger [4] is actually a simple spatial weighted average method, where the weights are determined by the normalized eigenvalues of the corresponding covariance matrix of the stacked images. However, along with simplicity there come several undesired side effects including contrast reduction.

© Lili Chen, Hongjun Guo, 2016

In frequency domain, the experts and scholars developed the multiscale decomposition (MSD) based fusion methods and achieved better fusion performance. The classical MSD methods include the discrete wavelet transform (DWT), the shift-invariant DWT (SIDWT), the nonsubsampled contourlet transform (NSCT) and the nonsubsampled shearlet transform (NSST) etc. Generally, there are three basic steps for MSD to fuse: 1) the source images are decomposed into multiscale representations in different scales and directions; 2) the multiscale representations are composited according to certain fusion rules; 3) the fused image is reconstructed using the corresponding inverse MSD transform [5]. However, no matter which one of the MSD is used, fusion cannot be achieved perfectly since MSD requires downsampling and upsampling during the decomposition and reconstruction process, and the original and reliable information of the source images may be changed to a certain degree. Besides, each MSD has its own drawbacks. For example, a common limitation of the DWT and SIDWT is that they cannot well represent the curves and edges of images since they lack directionality; the curvelet and contourlet transforms are shift-invariant, which are the same as the DWT [1]; the excellent performance of the NSCT and NSST is achieved at the cost of increasing computational complexity and memory, which is not suitable for surveillance image fusion due to their time-consuming property.

Surveillance applications usually involve continuous real-time monitoring, and the major challenge is to reduce computational complexity while preserving the fusion quality. Therefore, the important question in surveillance applications is how to improve the fusion speed [1].

Nowadays, compressed sensing (CS) is widely used for simultaneous data sampling and compression [6]. The CS principle provides the potential of dramatic reduction of samplinxg rates, power consumption and computational complexity in signal processing [6]. Inspired by this superiority, a novel surveillance image fusion method based on CS in spatial domain is proposed.

The rest of this paper is organized as follows. Section 2 presents the basic sampling theory of the CS, and then introduces the block-based sampling method; at last it proposes a modified version of the block-based sampling for fusion. In Section 3, a simple spatial domain fusion framework based on the two form of block-based sampling is proposed. Experimental results and conclusion are demonstrated in Section 4 and Section 5 respectively.

**Block-based CS sampling and a modified version.** Most existing works of CS are not suitable for real-time applications since the sampling process requires accessing the entire image at once.

Gan [6] proposed a bock-based CS sampling (BCSS) technique for fast CS, where the original image is divided into small distinct blocks and each block is sampled independently using the same measurement matrix in a low sampling rate. For simplicity, we term this divided block scheme the basic-BCSS or distinct-BCSS, and its schematic diagram is shown in Fig. 1. The main advantages of the basic-BCSS include: 1) measurement operator can be easily stored and implemented through a random undersampled filter bank; 2) block-based measurement is more advantageous for real-time applications since the encoder does not need to send the sampled data until the whole image is measured; 3) each block is processed independently.

Let us consider an $I_r \times I_c$ image $X$ with $N = I_r \times I_c$ pixels in total and suppose we want to take $n$ CS measurements. In the basic-BCSS, the image is divided into small distinct blocks with size of $B \times B$ each and sampled with the same operator. Let $x_i$ represent the vectorized signal of the $i$-th block through raster scanning, the corresponding output CS vector $y_i$ can be written as

$$y_i = \Phi_B x_i,$$

where $\Phi_B$ is an $n_B \times B^2$ orthonormalized i. i. d matrix with $n_B = \left\lfloor \frac{nB^2}{N} \right\rfloor$.

On the basis of the basic-BCSS, a modified BCSS is proposed in this paper, which is termed sliding-BCSS and shown in Fig. 1. In the sliding-BCSS, the image $X$ is divided into small sliding blocks instead, where $X$ is appropriately padded by repeating border elements

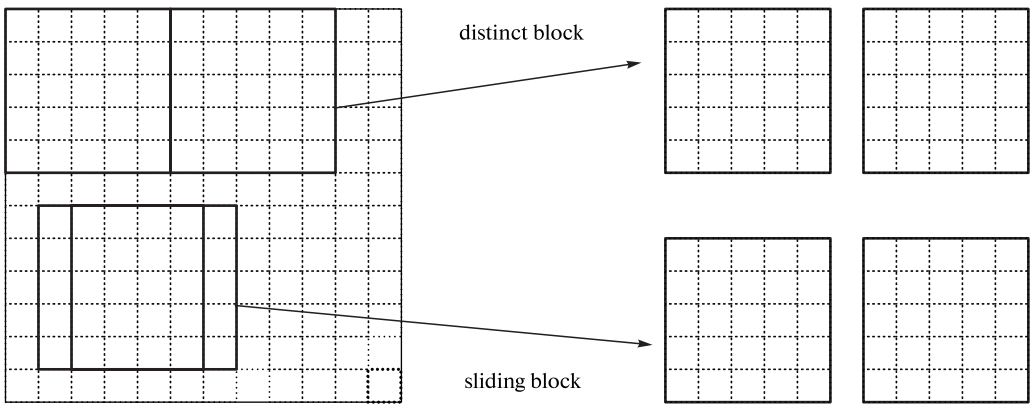


*Fig. 1. The schematic diagram of distinct block and sliding block*

in advance. Let us suppose that $x_{i,j}$ is a vector representing the sliding block centered on the location $(x, y)$, then the measurement result can be written as

$$y_{i,j} = \Phi_B x_{i,j}.$$

The other parameters are the same as before.

The advantages are: 1) the measurement result of each sliding block can be utilized to describe the feature of the specific pixel quantitatively since each pixel is correlative to its surrounding; 2) the measurement matrix is conveniently stored and employed because of its compact size [7].

**Fusion framework.** In this section, a simple and efficient spatial domain fusion framework is proposed for surveillance images. A fused image $F$ is assumed to be composed of a pair of the original source images $A$ and $B$ that have already been registered perfectly. The fusion framework consists of the following essential stages.

1. Obtaining the measurements of $A$ and $B$ using the basic-BCSS or sliding-BCSS.

2. Calculating the $L_2$-norm of the measurement for each block or pixel as the significance.

3. Generating a decision map through comparing the significances with the same location to form the fused image $F$ in spatial domain.

This fusion framework is essentially presented by two proposed fusion methods.

**Experimental results.** In this section, three pairs of grayscale surveillance images shown in Fig. 2, *a, b*, Fig. 4, *a, b* and Fig. 5, *a, b* are provided to demonstrate the validity and effectiveness of the two proposed fusion methods. All the images to be fused have been geometrically registered, which can be downloaded on the websites http://imagefusion.org and http://www.ece.lehigh.edu/SPCRL/IF/cwd.htm. These images have 256 grayscales and have different sizes. All the experiments are conducted in Matlab 8.5 on a PC with Intel Core 2.4GHz i3-4000M CPU and 4.00GB RAM.

Apart from the proposed fusion methods, several different traditional methods are also used in this paper. All the fusion methods are listed as follows.

(M1) SA fusion method [4].

(M2) PCA based fusion method [4].

(M3) DWT based fusion method [4].

(M4) SIDWT based fusion method [4].

(M5) NSCT based fusion method.

(M6) NSST based fusion method.

(M7) The proposed fusion method based on basic-BCSS.

(M8) The proposed fusion method based on sliding-BCSS.

In the above DWT, SIDWT, NSCT and NSST based fusion methods, all the decomposition levels are 3, and all the fusion rules are the average scheme for lowpass subbands and the maximum choosing scheme for highpass subbands. The wavelets used in DWT, SIDWT and NSST are DBSS(2, 2), Haar and 'maxflat', respectively, and the wavelets in NSCT are '9-7' for the pyramid filter and 'pkva' for the directional filter.

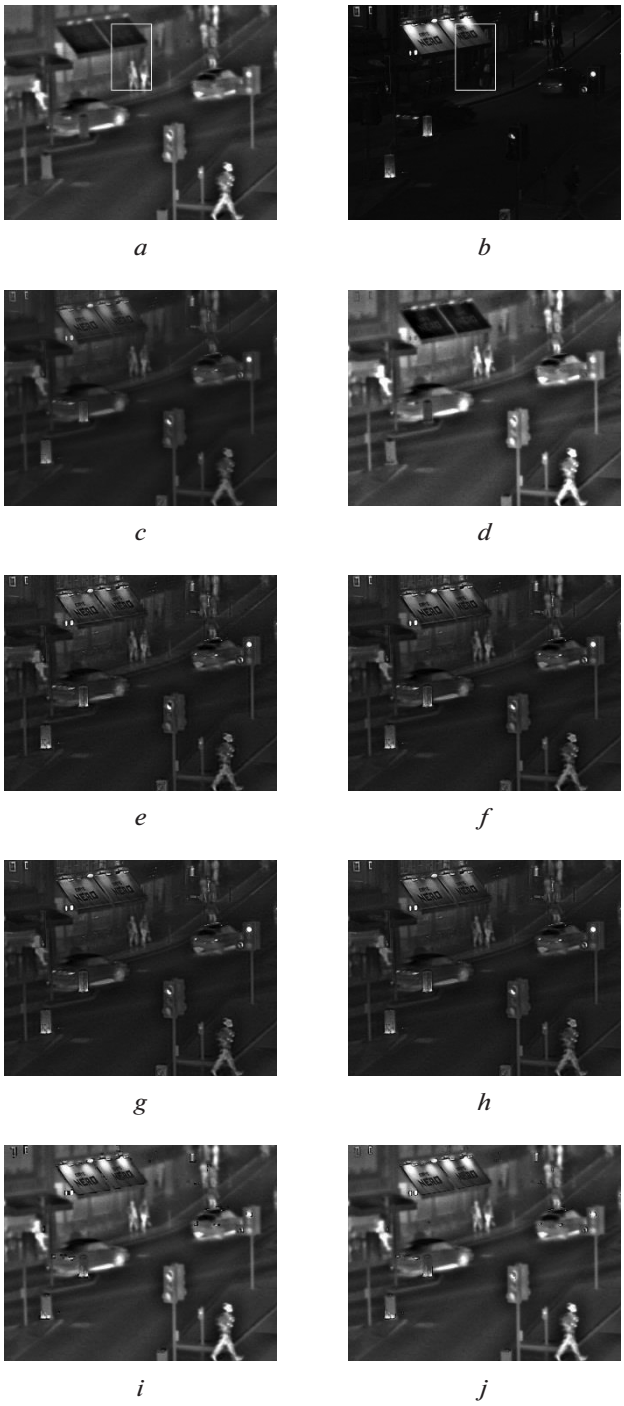

*a* *b* *c* *d* *e* *f* *g* *h* *i* *j*

*Fig. 2. 'Quad' infrared and visible images and the fused images:*

*a — infrared image; b — visible image; c—j — the fused images using M1—M8, respectively*

For evaluating the performance of the proposed fusion methods, several experiments are designed and the computed fusion results are compared by visual effect subjectively and quantitative image criteria objectively.

The visual effect analysis mainly focuses on the quality of the preservations and improvements of important image features and the overall image contrast, brightness and saturation.

The first experiment is performed on 'quad' infrared and visible images with a size of $496 \times 632$ shown in Fig. 2, *a, b*. From the source images, one can see that the images contain much complementary information. The visible image is only sensitive to the light, and almost all objects are invisible in the image. The entire image looks dark so that the image lacks brightness and contrast. The infrared image is sensitive to the difference of temperature, the pedestrians, the cars and the traffic lights have great contrast in the images. The resultant fused images based on M1–M8 are shown in Fig. 2, *c–j*. From the fused images, we can easily find that: 1) Fig. 2, *c* obtained by M1 has the lowest contrast without suspense; 2) Fig. 2, *d* obtained by M2 has pretty much the same appearance as the source infrared image, and the information of the source visible image is not transferred to the fused image at all, which indicates that M2 is with the worst fusion performance in this experiment; 3) Fig. 2, *e–h* obtain almost the same fusion effect, which are obviously better than Fig. 2, *c, d*. However, the images have low brightness and saturation, and the contrast is reduced to a certain extent, which are not suitable for human to perceive; 4) Fig. 2, *i, j* have approximately the equivalent results, where the most image features are conducted, and the images have the same brightness and saturation as the source infrared image.

For a clearer comparison, Fig. 3 depicts the details of the enlarged areas extracted from the images of Fig. 2, where the extracted area is shown in Fig. 2*, a, b*. It can be seen that the fused image obtained by M8 is with the best visual quality since almost all the useful information of the source images has been transferred to it, and it preserves the high contrast and brightness, which makes the objects very prominent for human observation. The fused image obtained by M7 is with the second best quality because it has certain block effects. Obviously, the block effects will become more serious as the block size increases. The block size used in M7 is $5 \times 5$. The performances of the other fused images are relatively poor, which is consistent with the previous discussion.

The second experiment is also performed on infrared and visible images. The source images 'kayak' are shown in Fig. 4, *a, b* with size of $510 \times 505$. Fig. 4, *a* is an AMB image captured by a Radiance HS infrared camera (Raytheon), and Fig. 4, *b* is a CCD image captured by Philips LTC500 CCD camera. Fig. 4*, c–j* show the fused images. Through visual observation, similar conclusion can be obtained, that is, the proposed two fusion methods provide the higher fusion performances.

The third experiment is performed on 'gun' MMW and visible images with size of $200 \times 256$ shown in Fig. 5, *a, b*. The MMW image is captured under 94 GHz millimeter-wave. As seen from the images, a concealed gun underneath the right person's clothing. The fused images are shown in Fig. 5, *c–j*, and Fig. 5, *i, j* provide the relative better performances with high contrast and brightness, which make it easy to identify the gun. The other images still have the sim-

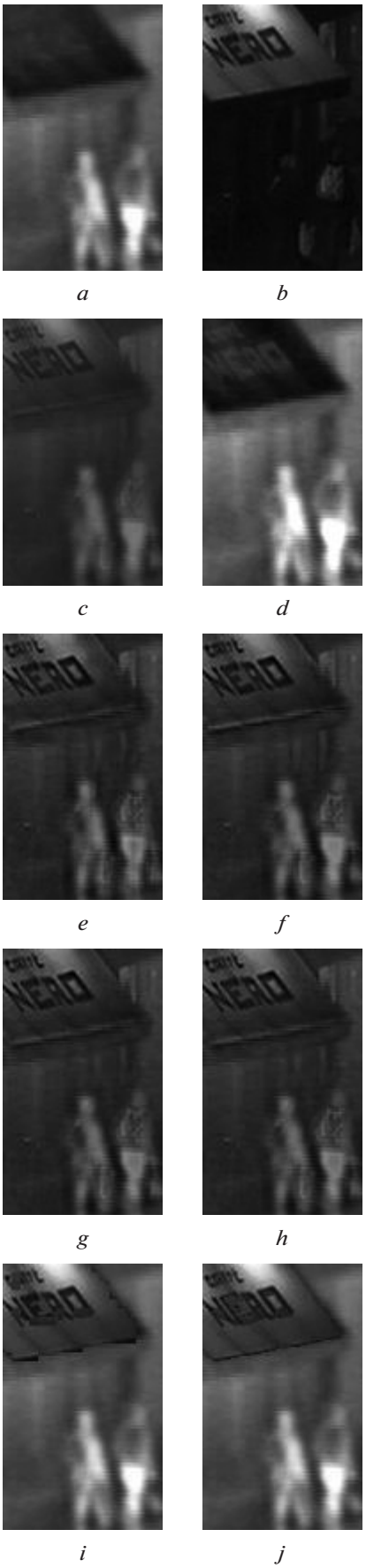


*Fig. 3. Detail of the enlarged areas:*
*a–j – the enlarged areas extracted from Fig. 2, a–j, respectively*

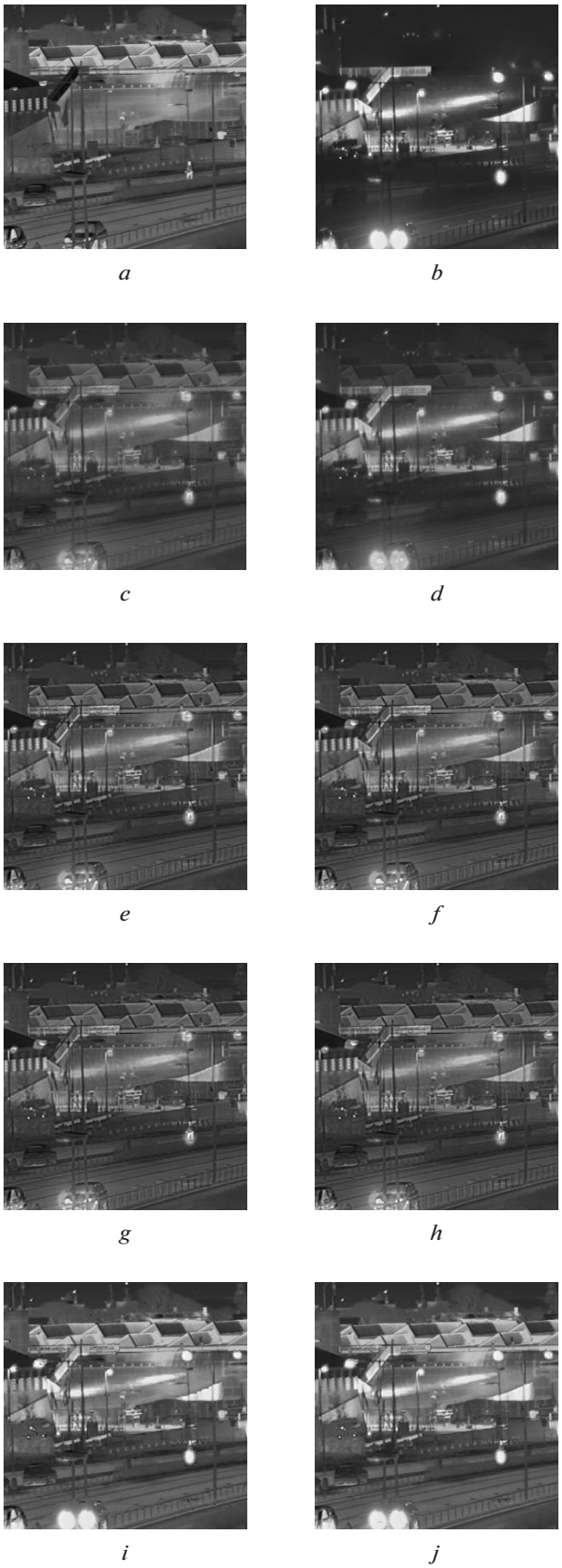

*a* *b* *c* *d* *e* *f* *g* *h* *i* *j*

*Fig. 4. 'Kayak' AMB and CCD images and the fused images:*

*a – AMB image; b – CCD image; c–j the fused images using M1-M8, respectively*

*a* *b* *c* *d* *e* *f* *g* *h* *i* *j*

*Fig. 5. 'Gun' MMW and visible images and the fused images:*

*a – MMW image; b – visible image; c–j the fused images using M1–M8, respectively*

ilar poor characteristics as in the first and second experiments.

To provide quantitative comparison of different fusion methods, the following image quality metrics are used in this paper: 1) standard deviation (SD), average gradient (AG), spatial frequency (SF) and information entropy (IE) are used to evaluate the spatial quality of the fused image; 2) correlation coefficient (CC), average error (AE) and mutual information (MI) are used to evaluate the relativity or difference between the fused image and one informative source image; 3) fea-

tured mutual information (FMI) [8], structural similarity image metric (SSIM) [9] and quality metric based on gradient (QAB/F) [10] are used to measure the degree of information transferred from the source images to the fused image. In addition, to measure the computational complexity of the fusion methods, the runtime (in seconds) of the corresponding Matlab fusion procedures is adopted as one fusion criterion, which is acquired by averaging the results of 10 times fusion procedure. Generally speaking, the larger the metrics values are, the better the fusion performance is, except for AE and the runtime.

The performance results of the three experiments are listed in Tables 1, 2, 3, respectively, where the best values are indicated in bold. As seen from the tables, there are two values shown in bold for each criterion because this paper refers to two proposed fusion methods. And according to the previous discussion of visual effect, M1 and M2 provide the poor fusion performance, so the corresponding data are not displayed in the tables. In the aspects of SD, CC, AE, AG, MI, SSIM and QAB/F metrics, the comparative performance of all the fusion methods is stable, and the two proposed fusion methods provide the best quality (the two methods have roughly the same performance). On the other hand, in the aspects of SF, IE and FMI metrics, despite the poor values occasionally, the two proposed methods still provide the best quality with larger probability. In the aspect of runtime metric, the DWT based fusion method is with the best values, and M7, one of the proposed methods, is with the second best values. The runtimes of M8 procedure are approximately the two times of that of M7, which results from the more blocks divided from the images and more computations to cost.

Overall, the fusion framework can provide the relatively perfect performance.

**Conclusion.** In this paper, a simple, effective and fast fusion framework using the basic-BCSS and the sliding-BCSS in spatial domain is proposed. Motivat-

*Table 1*

Quantitative results of fusion performance of the first ‘quad’ experiment

| Method | SD | AG | SF | IE | CC | AE | MI | FMI | SSIM | QAB/F | runtime |
|---|---|---|---|---|---|---|---|---|---|---|---|
| M3 | 0.0919 | 0.0296 | 0.0490 | 6.0317 | 0.7033 | 0.1282 | 1.0211 | 0.9190 | 0.7682 | 0.5290 | **0.0891** |
| M4 | 0.0952 | 0.0307 | 0.0488 | 6.0780 | 0.7193 | 0.1284 | 1.1198 | **0.9210** | 0.7867 | 0.6062 | 0.3013 |
| M5 | 0.0908 | 0.0292 | 0.0482 | 6.0054 | 0.7057 | 0.1281 | 1.0833 | **0.9211** | 0.7778 | 0.5588 | 147.4756 |
| M6 | 0.0903 | 0.0291 | 0.0482 | 6.0018 | 0.7063 | 0.1280 | 1.0915 | 0.9209 | 0.7778 | 0.5525 | 6.9346 |
| M7 | **0.1411** | **0.0479** | **0.0508** | **6.7898** | **0.8425** | **0.0138** | **4.3262** | 0.9163 | **0.9428** | **0.7002** | **0.2023** |
| M8 | **0.1409** | **0.0479** | **0.0533** | **6.7835** | **0.8455** | **0.0135** | **4.3263** | 0.9157 | **0.9429** | **0.7002** | 0.4375 |

*Table 2*

Quantitative results of fusion performance of the second ‘kayak’ experiment

| Method | SD | AG | SF | IE | CC | AE | MI | FMI | SSIM | QAB/F | runtime |
|---|---|---|---|---|---|---|---|---|---|---|---|
| M3 | 0.1317 | 0.0474 | 0.0501 | 6.9531 | 0.6906 | 0.0898 | 0.7922 | 0.8797 | 0.8050 | 0.5816 | **0.0739** |
| M4 | 0.1335 | 0.0481 | 0.0498 | 6.9620 | 0.6928 | 0.0905 | 0.8601 | **0.8843** | 0.8168 | 0.6389 | 0.2494 |
| M5 | 0.1297 | 0.0466 | 0.0484 | 6.9281 | 0.6943 | 0.0890 | 0.8289 | 0.8826 | 0.8197 | 0.6080 | 121.5679 |
| M6 | 0.1293 | 0.0465 | 0.0484 | 6.9241 | 0.6940 | 0.0889 | 0.8285 | 0.8818 | 0.8183 | 0.6015 | 5.9640 |
| M7 | **0.1692** | **0.0617** | **0.0516** | **7.2599** | **0.7212** | **0.0452** | **3.4752** | 0.8820 | **0.8209** | **0.6704** | **0.1785** |
| M8 | **0.1687** | **0.0615** | **0.0509** | **7.2501** | **0.7208** | **0.0453** | **3.4798** | **0.8867** | **0.8253** | **0.6730** | 0.3624 |

*Table 3*

Quantitative results of fusion performance of the third ‘gun’ experiment

| Method | SD | AG | SF | IE | CC | AE | MI | FMI | SSIM | QAB/F | runtime |
|---|---|---|---|---|---|---|---|---|---|---|---|
| M3 | 0.1113 | 0.0433 | **0.1374** | 5.8432 | 0.6999 | 0.0835 | 0.4082 | 0.7990 | 0.3262 | 0.5906 | **0.0160** |
| M4 | 0.1115 | 0.0435 | **0.1349** | 5.7846 | 0.7234 | 0.0809 | 0.4635 | 0.8063 | 0.3395 | 0.6471 | 0.0305 |
| M5 | 0.1076 | 0.0421 | 0.1323 | **5.8564** | 0.7133 | 0.0814 | 0.4419 | 0.8058 | 0.3489 | 0.6302 | 24.2515 |
| M6 | 0.1072 | 0.0419 | 0.1329 | **5.8626** | 0.7121 | 0.0815 | 0.4399 | 0.8064 | 0.3499 | 0.6252 | 0.8689 |
| M7 | **0.1461** | **0.0557** | 0.1315 | 4.3700 | **0.7485** | **0.0806** | **1.1523** | **0.8152** | **0.3845** | **0.7408** | **0.0862** |
| M8 | **0.1458** | **0.0556** | 0.1322 | 4.3734 | **0.7488** | **0.0807** | **1.1580** | **0.8203** | **0.3800** | **0.7297** | 0.1221 |

ed by the real-time requirement of surveillance applications and the superiority of low sampling basic-BCSS technique is firstly investigated, and then a modified version, namely sliding-BCSS, is put forward. The fusion framework mainly adopts the idea of selection scheme which is widely used in a fusion process. The experiments are performed on three pairs of surveillance images. Compared with traditional SA, PCA, DWT, SIDWT, NSCT and NSSCT based fusion methods; the fusion framework provides the relatively perfect performance with high contrast and brightness in visual effect and better values in quantitative criteria. Moreover, the fusion framework has low computational complexity, and it has a certain practical meaning for real-time surveillance applications.

**Acknowledgements.** This work was supported by Open Project of Intelligent Information Processing Lab at Suzhou University of China (No. 2013YKF17), Horizontal Project at Suzhou University of China (No. 2015h x 025) and Quality project of Anhui Province: Software engineering teaching team (2015jxtd041).

**References / Список літератури**

**1.** Li, S., Kang, X., Fang, L., Hu, J. and Yin, H., 2016. Pixel-level image fusion: A survey of the state of the art. Information Fusion, Vol. 33, pp. 100–112.
**2.** Adu, J., Gan, J., Wang, Y. and Huang, J., 2013. Image fusion based on nonsubsampled contourlet transform for infrared and visible light image. Infrared Physics & Technology, Vol. 61, pp. 94–100.
**3.** Hu, D., Shi, H., and Jiang, W., 2016. Infrared and visible image fusion using multiscale top-Hat transform and modified adaptive dual-channel pcnn. Revista Tecnica De La Facultad De Ingenieria Universidad Del Zulia, Vol. 39, No. 3, pp. 173–180.
**4.** Oliver Rockinger image fusion toolbox. [online] Available at: <http://www.metapix.de/toolbox.htm>.
**5.** Li, C., Ye, H., and Ye, J., 2016. Image fusion based on curvelet transform and principal component analysis. Revista Tecnica De La Facultad De Ingenieria Universidad Del Zulia, Vol. 39, No. 1, pp. 392–396.
**6.** Gan, L., 2007. Block compressed sensing of natural images. In: Proc. 15th International conference on digital signal processing, pp. 403–406.
**7.** Mun, S. and Fowler, J. E., 2009. Block compressed sensing of images using directional transforms. In: Proc. 16th IEEE international conference on image processing, pp. 3021–3024.
**8.** Haghighat, M. B. A., Aghagolzadeh, A. and Seyedarabi, H., 2011. A non-reference image fusion metric based on mutual information of image features. Computers & Electrical Engineering, Vol. 37, No. 5, pp. 744–756.
**9.** Wang, Z., Bovik, A. C., Sheikh, H. R. and Simoncelli, E. P., 2004. Image quality assessment: from error visibility to structural similarity. IEEE transactions on image processing, Vol. 13, No. 4, pp. 600–612.
**10.** Petrovic, V. and Xydeas, C., 2005. Objective image fusion performance characterization. In: Proc. 10th IEEE International Conference on Computer Vision, Vol. 2, pp. 1866–1871.

**Мета.** З метою вирішення проблеми злиття зображень спостереження в даній роботі пропонується простий та ефективний фреймворк злиття з використанням блочного стиснення вимірювань (BCSS), що складається з двох методів синтезу з використанням базового BCSS і ковзаючого BCSS відповідно.

**Методика.** За переваги низької частоти дискретизації та низької вимірювальної складності, в обробці сигналів широко використовується теорія стискування вимірів (CS). Основний алгоритм BCSS представляє собою базовий варіант блочного CS, в якому вихідне зображення розділяється на окремі блоки, а ковзаючий BCSS є модифікованою версією базового BCSS, запропонованого раніше, в якому зображення ділиться на невеликі ковзаючі блоки для кожного пікселя з відповідним відступом. Основна ідея фреймворка злиття полягає у виборі блоків чи пікселів з великою L2-нормою BCSS результатів вимірювань розділених блоків у просторовій області.

**Результати.** Фреймворк злиття протестовано на трьох парах зображень у відтінках сірого, у тому числі інфрачервоному та видимому зображеннях, міліметровому та видимому зображеннях, і проведене порівняння з декількома традиційними методами синтезу. Експериментальні результати показують, що запропонований фреймворк злиття може одночасно значно покращити якість злиття та швидкість.

**Наукова новизна.** Уперше запропоновано простий та ефективний фреймворк злиття з використанням BCSS у просторовій області.

**Практична значимість.** Результат має практичне значення для відеоспостереження в режимі реального часу.

**Ключові слова:** *злиття зображень, просторова область, спостереження, інфрачервоний, блочне стискування вимірювань, режим реального часу*

**Цель.** С целью решения проблемы слияния изображений наблюдения в данной работе предлагается простой и эффективный фреймворк слияния с использованием блочного сжатия измерений (BCSS), который состоит из двух методов синтеза с использованием базового BCSS и скользящего BCSS соответственно.

**Методика.** При перевесе низкой частоты дискретизации и низкой вычислительной сложности, в обработке сигналов широко используется теория сжатия измерений (CS). Основной алгоритм BCSS представляет собой базовый вариант блочного CS, в котором исходное изображение разделяется на отдельные блоки, а скользящий BCSS является модифицированной версией базового BCSS, предложенного ранее, в котором изображение делится на небольшие скользящие блоки для каждого пикселя с соответствующим отступом. Основная идея фреймворка слияния заключается в выборе блоков или пикселов с боль-

шой L2-нормой BCSS результатов измерений разделенных блоков в пространственной области.

**Результаты.** Фреймворк слияния протестирован на трех парах изображений в оттенках серого, в том числе инфракрасном и видимом изображениях, миллиметровом и видимом изображениях, и проведено сравнение с несколькими традиционными методами синтеза. Экспериментальные результаты показывают, что предлагаемый фреймворк слияния может одновременно значительно улучшить качество слияния и скорость.

**Научная новизна.** Впервые предложен простой и эффективный фреймворк слияния с использованием BCSS в пространственной области.

**Практическая значимость.** Результат имеет практическое значение для видеонаблюдения в режиме реального времени.

**Ключевые слова:** *слияние изображений, пространственная область, наблюдение, инфракрасный, блочное сжатие измерений, режим реального времени*

*Рекомендовано до публікації докт. техн. наук В. В. Гнатушенком. Дата надходження рукопису 25.12.15.*